Efficacy of Data-Driven Respiration Compensation Methods in fMRI Data at 1.5T

S. Hu[1], A. D. Kothari[1], Thomas M. Talavage[1,2]

[1]School of Electrical and Computer Engineering, Purdue University, West Lafayette, IN

[2]Department of Biomedical Engineering, Purdue University, West Lafayette, IN

INTRODUCTION

A significant component of noise in fMRI experiments arises from fluctuations in the static magnetic field produced by changes in the bulk susceptibility of the abdomen as a result respiration. Respiration noise compensation techniques seek to increase the CNR of small amplitude temporal fMRI signals for accurate detection of underlying neural activity. This work seeks to identify those circumstances in which compensation techniques are beneficial. A complex-valued image space algorithm and a magnitude-only filtering technique were assessed for improvements (relative to no compensation) in true and false detections of human baseline fMRI data with different rates of synthetic activation.

METHODS

Subjects

Two healthy adults were imaged in a dark room while wearing earplugs. Subjects were instructed to relax, remain motionless and respire naturally.

Imaging Parameters

- 1.5T GE (Milwaukee, WI) Signa CVi imager
- 20x20 cm FOV, 64x64 matrix, slice thickness of 5 mm
- Three experiments per subject, one imaging plane per experiment
- 512 images of each of 5 slices were acquired in axial, sagittal, and coronal planes
- Blipped echo-planar sequence (TR/TE = 360 ms/40ms).

Synthetic Activation

Known block paradigm activity was added to a 10x10 voxel region of the middle three slices. Each experiment was modified using activation rates ranging from 2-28 cycles per minute at contrast-to-noise ratios (CNRs) of 0.2 and 0.5.

Compensation Evaluation

The number of true and false detections (TD and FD) over the three slices was computed for each combination of rate and CNR in three cases:

(a) without compensation, Raw

(b) using complex image-space based waveform estimation and removal procedure [1], Cpx.

(c) using Gaussian-shaped magnitude-only band-reject filter centered at respiration rate [2], Gss

Detections were declared based on z-score thresholds of 1, 2 and 3. Confidence in observed activation was assessed by computing the empirical conditional probability of true detection given detection, p(T|D) = TD/(TD+FD), at each z-score threshold.

RESULTS

Effects of compensation procedure on TD and FD, aggregated over all three imaging planes, are shown in Figures 1 and 2. Subject respiration rates were post-hoc estimated at 18 breaths per minute for subject 1 and 16 breaths per minute for subject 2. Note that the number of possible TD and FD is 1800 and 71928 respectively.

When the rate of stimulus presentation matched the rate of respiration, a comparison of Cpx and Raw shows that Cpx produced

- at z>1: 52.5% fewer FD and 2.7% fewer TD
- at z>2: 70.4% fewer FD and 9.2% fewer TD
- at z>3: 86.5% fewer FD and 21.5% fewer TD

Data is aggregated over both subjects and CNR values. The band-reject filter Gss eliminated most TD as well as FD at z>1, and removed TD and FD completely at higher thresholds.

Figures 3 and 4 show the empirical probability of true detection given detection for subject 1 and 2, respectively. Each graph shows two different activation rates: one below and one at (or very near) the respiration rate of the subject.

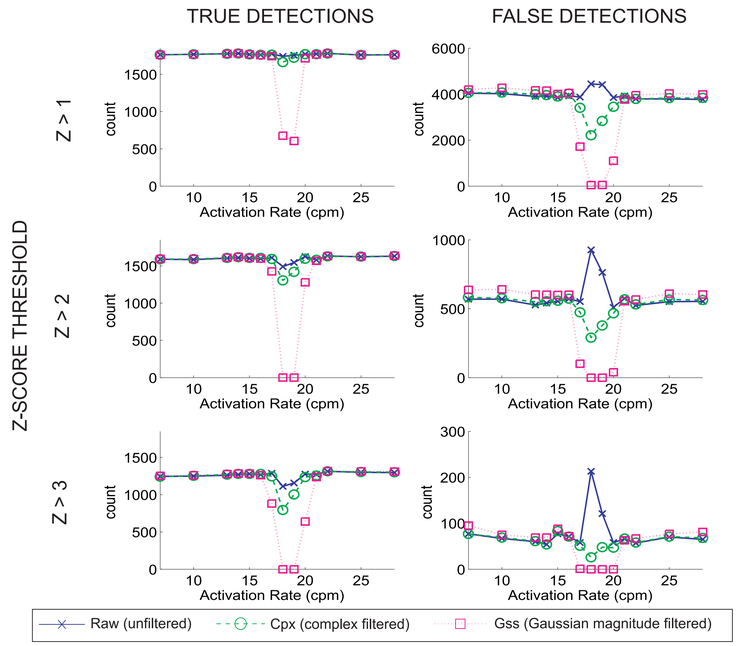

Fig. 1: Plot of true detections (TD) and false detections (FD) at z-score thresholds of z > 1, z > 2, and z > 3, for subject 1. When the rate of stimulus presentation matched subject 1's respiration rate (18 cpm), Gss eliminated almost all TD. Cpx removed some TD compared to Raw, but produced a large concomitant decrease in FD. When the stimulus presentation rate did not overlap the respiration noise bandwidth, all methods produced similar TD and FD compared to Raw, implying there was no benefit in performing respiration noise compensation. Maximum possible TD is 1800 and maximum possible FD is 71928.

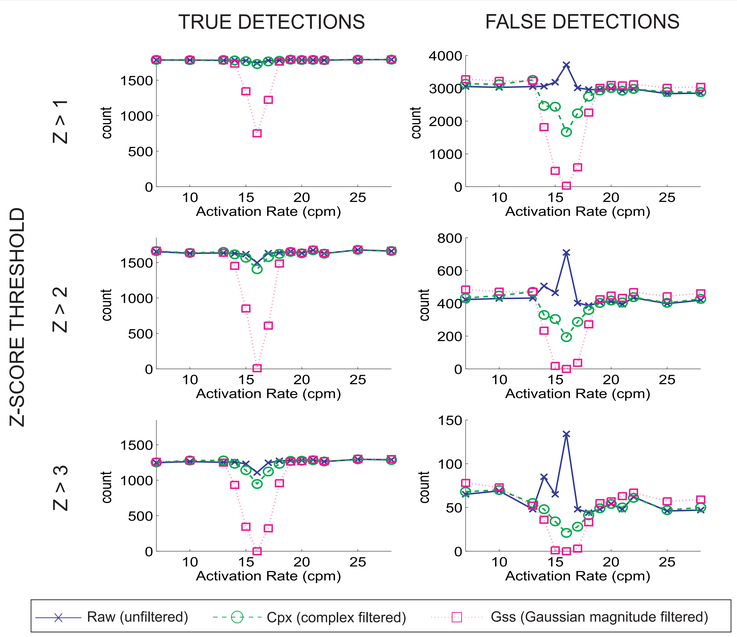

Fig. 2: Plot of true detections (TD) and false detections (FD) at z-score thresholds of z > 1, z > 2, and z > 3, for subject 2. When the rate of stimulus presentation matched the subject's respiration rate (16 cpm), Cpx produced minimal loss of TD with appreciable reduction in FD.

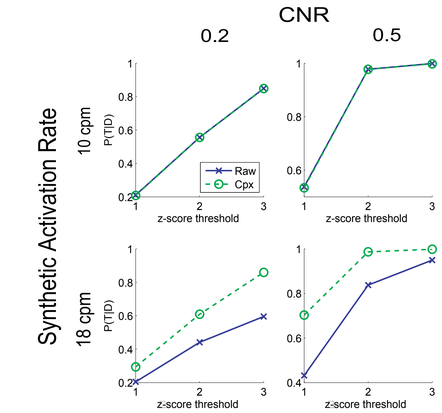

Fig. 3: Comparison of p(T|D)=TD/(TD+FD) for Raw and Cpx at activation rates (top) away from or (bottom) at the respiration rate of subject 1 (18 cpm). The specificity of detection for Cpx is greater than Raw when the activation rate matched the respiration rate, but is almost the same when the activation rate was away from the respiration rate.

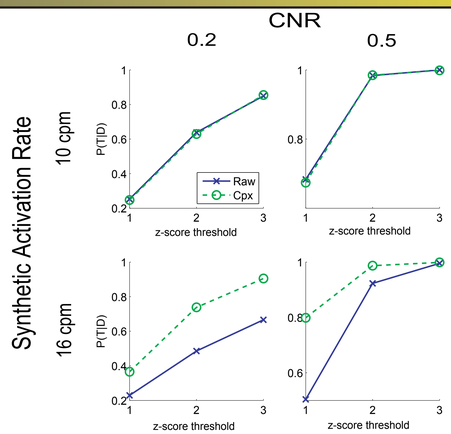

Fig. 4: Comparison of p(T|D) for Raw and Cpx at activation rates (top) away from and (bottom) at the respiration rate for subject 2 (16 cpm).

DISCUSSION

- When the activation rate is near the respiration rate, Cpx resulted in better specificity of detection by producing a large decrease in FD with a small concomitant decrease in TD compared to Raw. The magnitude-only filter (Gss) removed almost all TD and thus is detrimental to the experimenter.

- When the activation rate is not near the respiration rate, the performance of the respiration noise compensation algorithms approached the performance of the unfiltered case. All compensation procedures resulted in slightly higher FD compared to Raw.

CONCLUSIONS

The complex image space algorithm produced significant benefits over magnitude-only filtering, in terms of the number of true detections and the specificity of detection when the activation rate is near the respiration rate. When activation and respiration rates are far apart, there is no compelling evidence that respiration noise compensation algorithms are beneficial.

REFERENCES

[1] Ziyan et al., Proc ISMRM, p.1407, 2002; [2] Biswal et al., MRM 35:107-113